Applied Catalysis B: Environmental 168-169 (2015) 220–227

Contents lists available at ScienceDirect

Applied Catalysis B: Environmental

journal homepage: www.elsevier.com/locate/apcatb

Characterization of self-humidifying ability of SiO_2-supported Pt catalyst under low humidity in PEMFC

Insoo Choi[a,b], Hyunjoon Lee[c], Kyoung G. Lee[b], Sang Hyun Ahn[a], Seok Jae Lee[b], Hyun-Jong Kim[d], Ho-Nyun Lee[d], Oh Joong Kwon[c,*]

[a] Department of Energy and Mineral Resources Engineering, Kangwon National University, 346 Jungang-ro, Samcheok, Gangwon-do 245-711, Republic of Korea
[b] Center for Nanobio Integration & Convergence Engineering (NICE), National Nanofab Center, 291 Daehak-ro, Yuseong-gu, Daejeon 305-806, Republic of Korea
[c] Department of Energy and Chemical Engineering, Incheon National University, 119 Academy-ro, Yeonsu-gu, Incheon 406-772, Republic of Korea
[d] Surface Technology Center, Korea Institute of Industrial Technology (KITECH), 7-47, Songdo-dong, Incheon 406-840, Republic of Korea

ARTICLE INFO

Article history:
Received 6 August 2014
Received in revised form
10 November 2014
Accepted 17 December 2014
Available online 19 December 2014

Keywords:
Pt nanoparticle
SiO_2
Composite
Polymer electrolyte membrane fuel cell
Low humidity
Electrochemical impedance spectroscopy

ABSTRACT

SiO_2-supported Pt composite catalyst was developed by ultrasonic technique, and applied as anode catalyst of PEMFC to improve the performance under non-humidified condition. Two different MEAs were prepared: one for adjusting Pt loading and the other for matching thickness to conventional Pt-only MEA. The characteristic tools, such as TEM, XPS, TGA, and FE-SEM were employed to characterize the composite catalyst and the MEAs thereof. The long-term performance of MEAs with the composite catalyst was evaluated under non-humidified and elevated temperature, and compared with that of Pt-only MEA. The self-humidifying ability of SiO_2-supported Pt catalyst was examined by EIS technique.

1. Introduction

Polymer electrolyte membrane fuel cell (PEMFC), also known as proton exchange membrane fuel cell, has been regarded as a new power source for portable devices and electric vehicles due to its promising attributes such as large power density, high fuel-to-energy conversion efficiency, and environmental advantage [1–6]. On this account, scientists and engineers have tried to develop the related technologies in order to make fuel cell commercially available.

The performance of PEMFC is dictated by the proton conductivity of the membrane electrode assembly (MEA); a combination of polymer electrolyte and catalyst layer [1–3,7–10]. Since the proton conductivity is proportional to the water content in the MEA [11,12], MEA should be sufficiently hydrated. A low-hydration state leads to the increase of resistance in membrane and catalyst layer, and ultimately results in performance loss [8–10]. In order to maintain the hydration level of MEA, fuel cell is externally supplied with water by pre-humidifying gaseous oxygen and hydrogen fuel. However, the external humidification is a burden for PEMFC system because it requires a large space for installation and considerable energy for heating [13]. Thus, the limited use of external humidification is desirable for PEMFC system.

In this regard, other methods to keep the MEA sufficiently hydrated than the external humidification are highly required for the economic and efficient operation of PEMFC. There have been three approaches reported so far. The first method is to grant self-humidifying ability to polymer membrane [7–10,14,15]. Watanabe et al. first proposed a self-humidifying electrolyte membrane, which was made by addition of nano-sized hygroscopic material; i.e., SO_2 [7], TiO_2 [8] into Nafion solution, followed by casting and incorporating Pt nanaocrystallites as a result of cation exchange treatment. Bocarsly et al., also reported silicon oxide/Nafion composite membrane, which was prepared either by impregnating

* Corresponding author at: Bldg. A, Room #564, Department of Energy and Chemical Engineering, Incheon National University, 119 Academy-ro, Yeonsu-gu, Incheon 406-772, Republic of Korea. Tel.: +82 32 835 8414; fax: +82 32 835 8423.
E-mail addresses: insoochoi.kr@gmail.com (I. Choi), vesperia@nate.com (H. Lee), kglee@nnfc.re.kr (K.G. Lee), news0826@gmail.com (S.H. Ahn), sjlee@nnfc.re.kr (S.J. Lee), hjkim23@kitech.re.kr (H.-J. Kim), hnlee@kitech.re.kr (H.-N. Lee), ojkwon@incheon.ac.kr, ohjoongkwon@gmail.com (O.J. Kwon).

http://dx.doi.org/10.1016/j.apcatb.2014.12.026
0926-3373/

polymer membrane via sol–gel process of tetraethylorthosilicate (TEOS) or by recasting film [14]. In both reports, the extents of hygroscopic materials in the composite membrane were less than or equal to 10 wt%, because the increase in the resistance of membrane was concerned, owing to the incorporation of non-proton-conductive material. There was an attempt by Bi et al., who prepared Nafion/SiO_2-sulfated zircornia membrane by solution-casting method to minimize the proton conductivity loss from addition of hygroscopic SiO_2 [15]. In addition, two-layer [16] or three-layer [17] composite membranes consisting of a layer of Pt catalyst dispersed in Nafion and a layer of recast Nafion membrane were proposed as well. Although improved performances were observed in these studies, the composite membrane left durability issue at elevated temperature. For instance, the non-homogeneous membranes would swell and expand at different extent, due to difference in water absorbing ability and thermal expansion coefficient.

The second approach is to fabricate a composite catalyst layer by mixing metal oxide with active metal catalyst [18,19]. The addition of SiO_2 [18] or Al_2O_3 [19] in the catalyst layer has been already reported, and it was confirmed that the performance increased owing to the enhanced wettability under low humidity condition. Jung et al., simply added commercially available SiO_2 nanoparticle (NP) into the anode and cathode catalyst layer, and measured the performance of MEA under different relative humidity [18]. The performance was improved when SiO_2 (weight fraction of SiO_2 based on Pt/C < 0.4) was added in the anode catalyst layer under low anode and cathode relative humidity, because SiO_2 assisted the absorption of water by external humidification and back diffusion. Moreover, Chao et al. sprayed γ-Al_2O_3 suspension up to 40 wt% on either anode and cathode side, and measured the performance of MEA [19]. At 10 wt% of γ-Al_2O_3 as an optimum, the performance was highest due to the balance between wettability and electrical resistance. However, the hygroscopic particles are easy to be detached or aggregated, because they are simply mixed in catalyst layer, or not immobilized in the catalyst layer. In this regard, the method cannot assure stable performance during long-term operation.

The last approach is to fabricate a self-humidifying composite catalyst made of metal catalyst and hygroscopic material [20,21]. Su et al. introduced amorphous SiO_2 in the composite catalyst by hydrolysis of TEOS [20]. The low humidity performance of Pt/SiO_2/C catalyst exhibited the highest at 10 wt% of SiO_2, and maintained it until the relative humidity decreased to 28%. Under that low humidity condition, MEA with Pt/SiO_2/C did not degrade, showing stability 120 h at 50 °C. The method not only includes all the advantages of using SiO_2 as the previous two methods do, but also immobilizes the hygroscopic material in the catalyst layer, giving additional durability. However, the durability confirmed in above study is not based on where PEMFC normally operates, which is above 65 °C. The study admitted that the low humidity performance of Pt/SiO_2/C was quite susceptible to the cell temperature, which decreased rapidly as the cell temperature increased from 50 to 70 °C. Therefore, the stable performance of self-humidifying catalyst should be confirmed under the real-life operation of PEMFC.

In our previous study, the authors reported that Pt-deposited SiO_2 nanocomposite catalyst (Pt/SiO_2—C) had been successfully fabricated through sonochemical reduction of Pt [21]. By varying the temperature of reactant gas, the performance of MEA with the nanocomposites at cell temperature of 70 °C under the specific relative humidity was presented. As a result, as synthesized catalyst could retain 87% of initial performance under the relative humidity of 39%. In this study, the authors attempt to confirm the durability of Pt/SiO_2—C for a long-term operation under non-humidified and elevated temperature condition, and to characterize its self-humidifying ability by analyzing electrochemical impedance spectroscopy (EIS). The EIS is widely used for diagnostic purposes for fuel cells under load with various operating condition, such as drying [22–26], flooding [22,26], and poisoning [26].

2. Experimental

2.1. Synthesis of composite catalyst

The synthetic process for monodisperse SiO_2 NP, with approximate size of 46 nm, was addressed in our previous result [21]. 24 mg of chloroplatinic acid hydrate (H_2PtCl_6•xH_2O, Sigma–Aldrich) was added to the SiO_2-dispersed aqueous solution (100 mg SiO_2 in 30 ml de-ionized water), and the ultrasonic irradiation was conducted to the mixture solution with power of 80 W/cm^2 for 15 min. 4 mL of ammonium hydroxide (NH_4OH, 28~30 v/v%, Sigma–Aldrich) was dropped into the mixture solution before applying ultrasound. Pt-deposited SiO_2 NPs (Pt/SiO_2) were washed with de-ionized water over times, centrifuged, and dried at 60 °C for overnight. Carbon black (2.5 mg, VulcanXC-72, Cabot corp.) was added to 10 mg of Pt/SiO_2. The weight ratio of carbon black out of the total was set to 0.20. The mixture was then thermally treated under the given atmospheric condition (H_2/Ar = 1:9) at 300 °C for 3 h. After cooled down, Pt/SiO_2 with conducting carbon (Pt/SiO_2—C) was collected. The synthesis of Pt/SiO_2—C was illustrated in Fig. S1.

2.2. Fabrication of MEA with composite catalyst

In this study, two different MEAs were prepared: a Pt mass-corrected MEA (MEA-M) and a thickness-corrected MEA (MEA-T). Both MEAs were fabricated by catalyst-coated membrane (CCM) method. MEA-M was prepared by following process. For anode, Pt/SiO_2—C ink was prepared by ultrasonic mixing of 10 mg of the composite catalyst with Nafion^{TM} perfluorosulfonic acid (PFSA) polymer dispersion (5 wt% polymer content, DE520, Dupont^{TM}); 1 ml of isopropyl alcohol (IPA, JUNSEI) with 68 μl of Nafion^{TM} solution. The anode catalyst was loaded on polymer membrane (NRE-212, Dupont^{TM}) by spraying coating, and Pt loading was 0.1 mg_{Pt} cm^{-2}. For cathode, commercial Pt/C (40 wt% Pt, Johnson Matthey) was used with same ink composition and preparation method, but 0.2 mg_{Pt} cm^{-2} of Pt loading on the other side of the membrane. Then, catalyst-coated membrane was sandwiched by the porous gas diffusion layers (GDL, 35BC with surface area of 6.25 cm^2).

MEA-T was prepared by the same as above but, the anode catalyst layer was formed via thickness calibration with respect to catalyst loading of Pt/SiO_2—C, which will be discussed later. The MEA, fabricated with commercial Pt/C (MEA-C) on both anode and cathode, was also prepared by identical process for comparison. The preparation of MEA and its assembly was depicted in Fig. S2.

2.3. Single-cell measurement, durability test, AC impedance analysis

Performance of MEA-M, MEA-T, and MEA-C were evaluated by integrated fuel cell station (custom-made, CNL). The experiment was performed in galvanostatic mode with current up to 2.8~3.4 A/cm^2. Reactant gases were pure H_2 (100 sccm) and O_2 (200 sccm) for anode and cathode, respectively, and fed through a humidifier. All MEAs were activated prior to the measurement (70 °C, 300 min). The performance was measured under fully humidified and non-humidified condition, in order to investigate the self-humidifying ability of composite catalysts, and to compare them to commercial Pt/C. The non-humidified condition was set

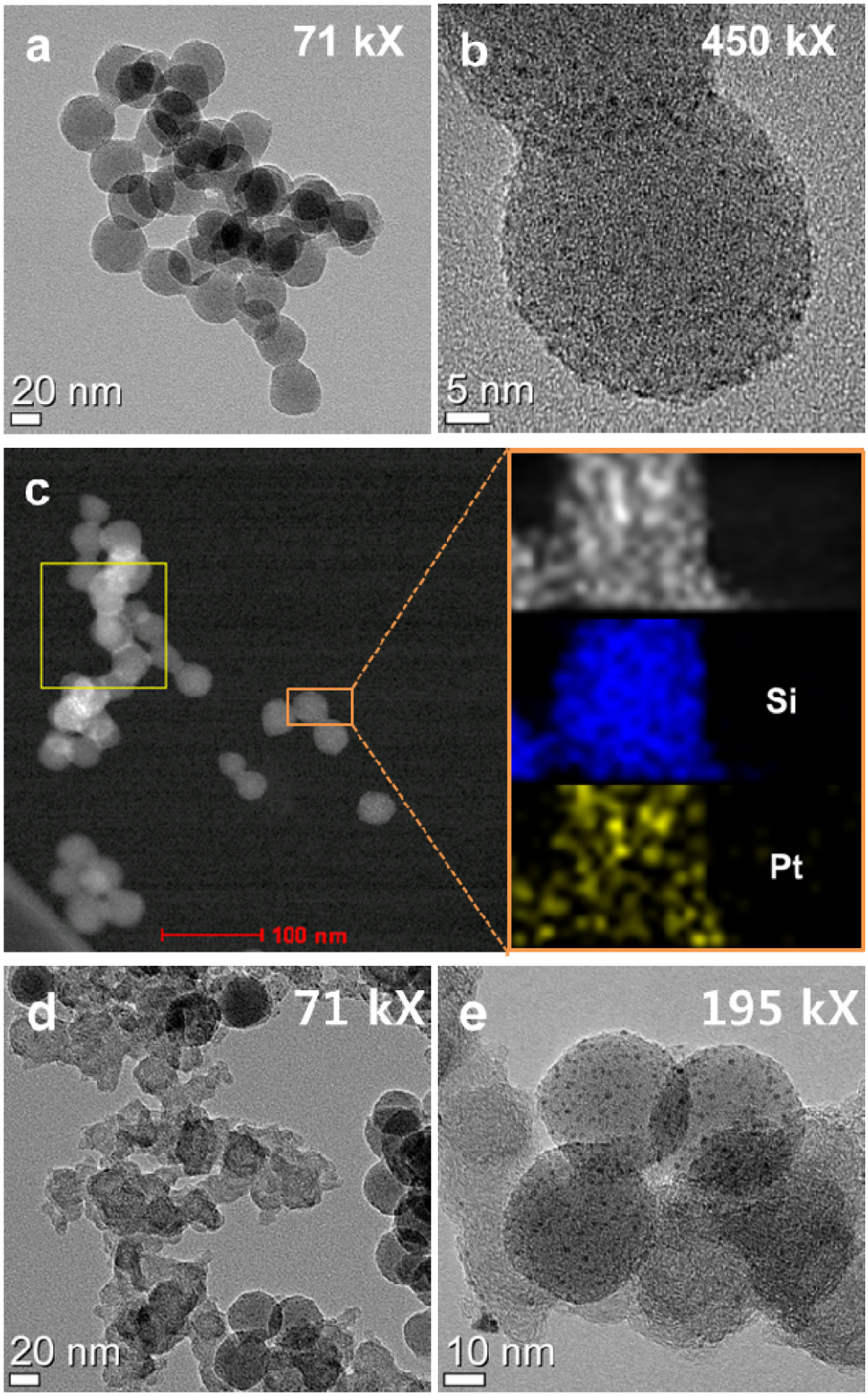

Fig. 1. TEM image of Pt/SiO_2 NPs; (a) 71 kX, (b) 450 kX, (c) STEM image with elemental mapping for Pt and Si in Pt/SiO_2, TEM image of Pt/SiO_2—C composite catalyst; (d) 71 kX, (e) 195 kX.

by flowing fuel gases into the cell without passing through the humidifier. The durability under the non-humidified condition was monitored in a span of 10 h at the current density of 0.2 A cm^{-2}.

EIS analysis was done in the potentiostatic mode by using potentiostat (PARSTAT 2273, PAR) when the cell was at thermodynamically steady state. The applied potential was 0.60 V, and the sweeping frequency ranged from 10 kHz to 1 Hz with 5 mV of AC signal amplitude.

2.4. Physicochemical characterization

X-ray photoelectron specrtroscopy (XPS, Ulvac, Al K-alpha) and transmission electron microscope (TEM, JEOL, 200 kV), equipped with energy dispersive X-ray (EDX) were used for confirming metallic Pt, and for quantitative analysis on the composite catalyst. Another TEM for analytical purposes (TEM, Tecnai, 200 kV) was employed for imaging the composite materials. The cross-section of MEA, and hence the thickness of catalyst layer was obtained from field emission secondary electron microscope (FE-SEM, JEOL). Before FE-SEM analysis, MEA was dipped into liquid nitrogen and broken into pieces to acquire the cross-section. Thermogravimetric analysis (TGA, PerkinElmer) of the composite catalyst provided the supplement result for carbon addition.

3. Results

3.1. Characterization of composite catalyst

The low and high magnified TEM images of the Pt/SiO_2 NP are shown in Fig. 1(a) and (b), respectively. It was observed that Pt NPs, with average size of 1.4 (±0.22) nm, were uniformly formed on the surface of SiO_2 sphere of which diameter was about 46 (±2) nm. The reduction of Pt ion was induced by cavitation effect, where micro-bubbles are formed upon ultrasound irradiation and collapse violently as pressure increases. When the bubble collapses, the shockwave is generated, dissociating water into $OH^{\bullet}$ and $H^{\bullet}$ radicals, which further act as reductants for formation of Pt NPs [27–29]. Meanwhile, the attachment of Pt NP and their immobilization onto SiO_2 surface could be explained well by the following. The bubbles near the solid surface oscillate non-spherically, and high velocity jet of liquid is directly toward the surface, which is called micro-jet phenomenon [29,30]. This micro-jet along with acoustic stream enabled the fixation of Pt NP on the SiO_2 surface. TEM-EDS mapping result in Fig. 1(c) confirmed the Pt NPs, the yellow scattered dots, over the SiO_2 surface. Pt/SiO_2—C composite catalyst was also imaged by TEM, as in Fig. 1(d) and (e). Irregular carbon black was well-mixed with Pt/SiO_2 NPs, and thus would provide a pathway for electro-conduction. Moreover, it seemed that Pt NP on the SiO_2 barely migrated to elsewhere, for instance to carbon black, even after the post-heat treatment. This assured the successful immobilization of Pt on SiO_2 surface via micro-jetting under ultrasound irradiation.

Pt/SiO_2—C composite catalyst after the heat treatment was analyzed by XPS. The metallic Pt was confirmed by the characteristic peaks ($Pt4f_{7/2}$ = 71.3 eV; $Pt4f_{5/2}$ = 74.5 eV) from XPS analysis given in Fig. S3(a). The weight percentage of Pt in Pt/SiO_2 was 11 wt%, confirmed by XPS quantitative analysis in Fig. S3(b), which was accordance with TEM-EDS results in Fig. S4. As already mentioned, high surface area carbon black was added to Pt/SiO_2 NPs for increasing electric conductivity of the composite catalyst. The mass ratio of newly-added carbon to the composite catalyst was measured to be 21.08 wt% from TGA result (Fig. S5), and therefore, Pt wt% in Pt/SiO_2—C was approximated to 8.68 wt%. The above composition of Pt/SiO_2—C was applied when MEA was fabricated.

3.2. Preparation of MEA with composite catalyst via calibration

The MEA-M was fabricated with Pt/SiO_2—C, having a corresponding Pt loading to the MEA-C. However, the use of composite catalyst created thick catalyst layer due to size, and hence high volume of SiO_2 NP. The increase in the catalyst layer causes the internal resistance to increase [31–33]. For the sense, another MEA with Pt/SiO_2—C (MEA-T) possessing equivalent thickness to MEA-C, was prepared and tested as well. Following is the process for the fabrication of MEA-T. First, the calibration of thickness to the catalyst loading was conducted in order to find the correlation between them. As confirmed in Fig. 2, the catalyst loading and the average thickness of the catalyst layer exhibited the 1st order linear correlation (R^2 = 0.997) as a result of the calibration. The thickening from using Pt/SiO_2—C compared to Pt/C was once more verified by FESEM-EDS analysis in Fig. S6. From this, the thickness of the catalyst can be predicted once the catalyst loading was known. The thickness of catalyst layer of Pt/C with 0.1 mg_{Pt} cm^{-2} was 2.3 μm. Based on the calibration curve, 2.45 mg of Pt/SiO_2—C was required to have corresponding thickness. The actual thickness of Pt/SiO_2—C in MEA-T was measured to be 2.7 μm, which approximated to the catalyst layer of Pt/C. The specification in terms of catalyst loading and layer thickness of MEA-M, MEA-T, and MEA-C are presented in Table 1.

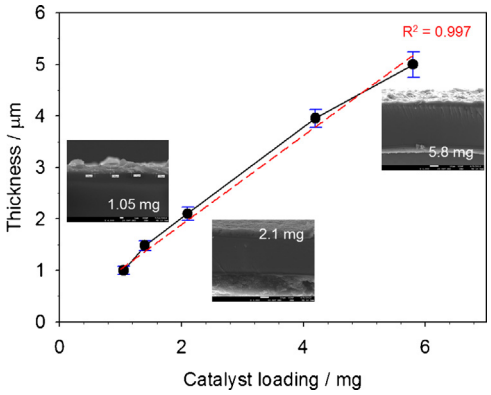

Fig. 2. Thickness calibration with respect to catalyst loading for Pt/SiO_2—C.

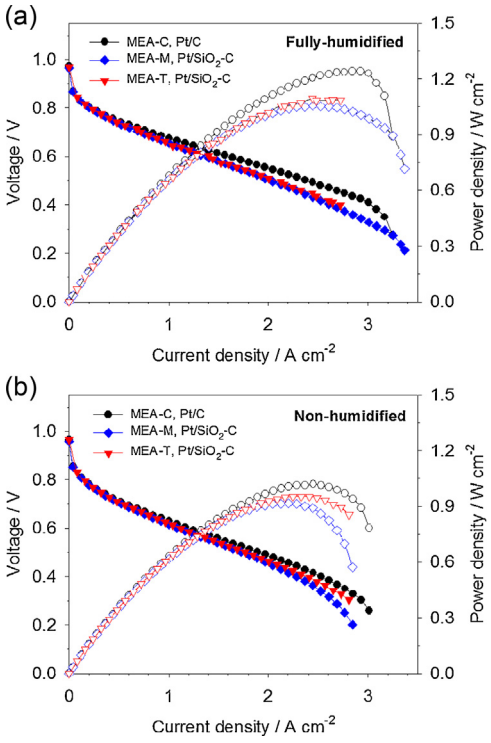

Fig. 3. Single cell i-V, i-P curve for MEA-C, MEA-M, and MEA-T under (a) fully-humified and (b) non-humidified condition.

Table 1
The specification of MEA-C, MEA-M, and MEA-T fabricated in this study.

Catalyst	Pt/C commercial	Pt/SiO_2 —C	
MEA	MEA-C 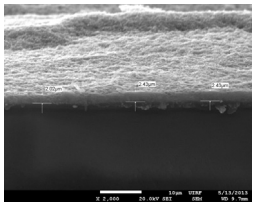	MEA-M 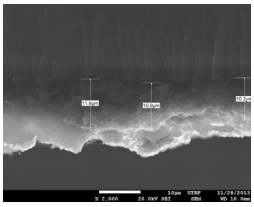	MEA-T 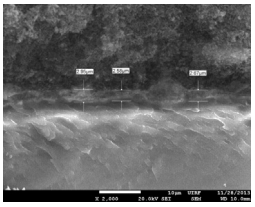
Loading mass	1.6 (0.1 mg_{pt}/cm^2)	7.55 (0.1 mg_{pt}/cm^2)	2.45 mg (0.0325 mg_{pt}/cm^2)
Anode thickness	2.3 μm (±0.2)	10.9 μm (±0.8)	2.7 μm (±0.2)

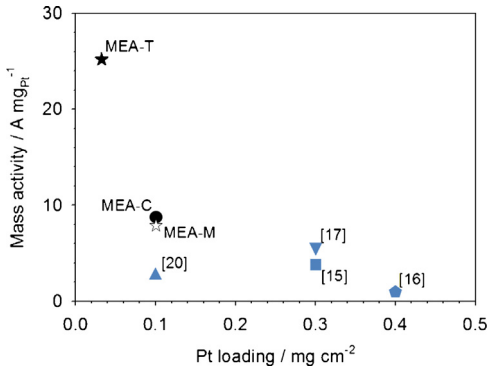

Fig. 4. The mass-activity of MEA-C, MEA-M, and MEA-T with comparison to references.

3.3. Single cell performance under humidified/non-humidified condition

The single cell performances of the three MEAs at 70 °C in fully-humidified and non-humidified condition were shown in Fig. 3. The normal operating voltage of PEMFC ranges from 0.6 to 0.7 V. For the sense, the current density and the power density at 0.65 V were compared and summarized in Table 2. At humidified and non-humidified state, the performance of both MEA-M and MEA-T were short of MEA-C. It was attributed to the increased resistance in catalyst layer owing to low conductive SiO_2 particles inside the composite catalyst. However, both MEAs exhibited the apparent self-humidifying ability, which was represented by the extent of decrease in current density from humidified state to non-humidified state. As seen in Table 2, MEA-C maintained about 71.8% of its initial performance in non-humidified condition, while MEA-M and MEA-T exhibited 76.9% and 80.3% of their initial performance, respectively. This is ascribed to the water-retaining property of SiO_2 NP in composite catalyst, which helped the MEA sustaining the humidity, and therefore retained protonic conductivity [18–21]. The contribution of SiO_2 to the humidification of MEA, a membrane and a catalyst layer, will be differentiated and addressed by using EIS technique in the following section.

It is of importance to notice that the mass-activity of these MEAs with the composite catalyst under non-humidified condition were higher than those from other studies, due to small amount of Pt in the composite. In Fig. 4, the mass-specific activity of MEA-T and MEA-M were compared to the others, previously reporting on the self-humidifying ability of different MEAs under less or non-humidified condition as seen in Fig. 4. Su et al. [20] performed low-humidity single cell operation with Pt/SiO_2 catalyst (0.1 $mg_{Pt}\,cm^{-2}$ for anode). Under RH 28%, the catalyst showed self-humidifying ability, however, the performance was far below from our study. In addition, Liu prepared Pt-CNT-Nafion reinforced self-humidifying MEA (0.3 $mg_{Pt}\,cm^{-2}$) for PEMFC, and operated it under dry condition. The performance was still short of what is shown in our study, and the Pt content was greater than ours. In our study, MEA-T possessed three times higher mass-activity than MEA-C when they were not humidified.

Amongst the composite-embedded MEAs, the MEA-T exhibited less polarization than MEA-M, and therefore showed higher current and power densities. It was also ascribed to the highly-resistant SiO_2, which occupied higher area-specific weight in the catalyst layer of MEA-M than of MEA-T (Fig. S7). Moreover, the activation loss of MEA-T was almost same with that of MEA-M, even though MEA-T contained less amount of Pt than MEA-M (0.0325 $mg_{Pt}\,cm^{-2}$ in MEA-T vs. 0.1 $mg_{Pt}\,cm^{-2}$ in MEA-M). The result indicated that Pt on SiO_2 was sufficiently utilized, and the severe activation loss was prevented. It can be further inferred that the Pt-deposited SiO_2 and carbon made a close network, and thus, three-phase boundary for the fuel cell reaction was efficiently established. Consequently, in terms of the performance and the Pt loading, MEA-T is more favored and appropriate as a self-humidifying catalyst than MEA-M. In this regards, the durability measurement and the evaluation of resistance under non-humidified condition was performed with MEA-T.

3.4. Durability of self-humidifying catalyst under non-humidified condition

The durability of self-humidifying catalyst under non-humidified condition and elevated temperature was evaluated by constant current operation for 10 h. Only the anode was in

Table 2
The current density (j) and power density (P) at 0.65 V of MEA-C, MEA-M, and MEA-T under humidified/non-humidified condition.

	MEA-C, Pt/C(0.1 $mg_{Pt}\,cm^{-2}$)	MEA-M, Pt/SiO_2—C(0.1 $mg_{Pt}\,cm^{-2}$)	MEA-T, Pt/SiO_2—C(0.0325 $mg_{Pt}\,cm^{-2}$)
	Fully humidified/Non-humidified		
j/A cm^{-2}	1.204/0.865	1.037/0.797	1.020/0.819
Δj/%*	−28.16	−23.11	−19.71
P/W cm^{-2}	0.783/0.563	0.675/0.518	0.663/0.533
ΔP/%**	−28.16	−23.23	−19.66

* Δj is calculated by $(j_{\text{non-humidified}} - j_{\text{fully humidified}})/j_{\text{fully humidified}} \times 100$.
** ΔP is calculated by $(P_{\text{non-humidified}} - P_{\text{fully humidified}})/P_{\text{fully humidified}} \times 100$.

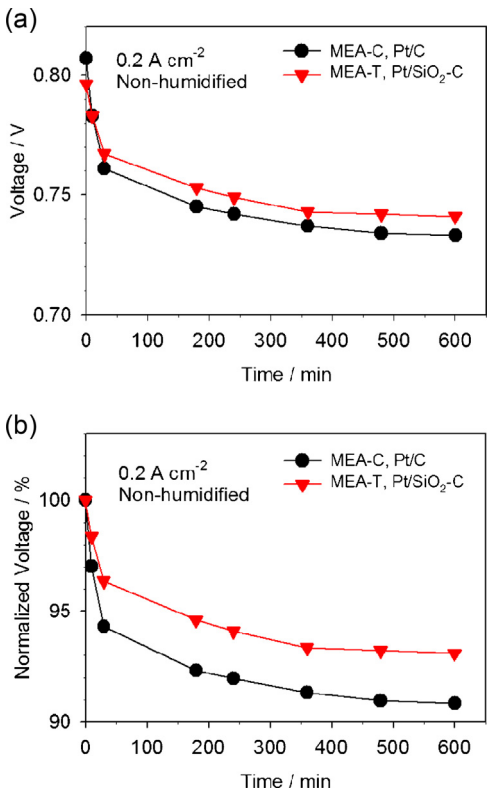

Fig. 5. (a) The voltage decay during drying time up to 600 min, with (b) normalized value for MEA-C and MEA-T.

non-humidified condition and the cathode was fully humidified, which made it certain that the cathode would not be a limiting factor on the performance of the MEA. Our purpose was to evaluate the self-humidifying ability of catalyst in anode which was apparently susceptible to dehydration. As being said, all measurement was performed with MEA-T, and the results were given with a comparison to MEA-C in Fig. 5. The voltage decay at 0.2 A cm^{-2} under non-humidified condition was monitored for 10 h. MEA-C maintained 90.83% of its initial performance, while MEA-T exhibited 93.09% of initial performance.

In this study, the decay amount of cell performance for both MEA-C and MEA-T with prolonged operation under non-humidified condition was relatively smaller than what have been reported in the other literature [22,23,26]. This was attributed to the different measurement scheme and relatively thin catalyst layers. In this study, all durability tests were conducted after the cells were activated, and therefore the water produced during the activation was still distributed in the catalyst layer. In addition, the catalyst layers were not so thick that extremely high resistances were applied. At any rate, the self-humidifying ability of the composite catalyst was definite during a long-term operation under non-humidified condition.

3.5. Characterization of self-humidifying ability of composite catalyst by EIS

The EIS could diagnose the lack of sufficient humidification of single cell, and hence the loss in cell performance by its change [2,3,22–26]. Three different factors are resolved in the impedance spectra: the membrane resistance, the resistance of the ionomeric component within the catalyst layer, and the interfacial impedance for the sluggish oxygen reduction reaction (ORR), by high-frequency (10^5~10^2 Hz) intercept at real-axis, mid-frequency (10^2 Hz~1 Hz) semi-circle, low-frequency (<1 Hz), respectively [34,35]. The spectra can tell the origin of dynamics in the single cell upon various reaction conditions.

The in-situ EIS spectra for MEA-C and MEA-T in non-humidified condition were presented in Fig. 6. The spectra were obtained with a time span of 10~480 min. The Nyquist plots for MEA-C and MEA-T were given in Fig. 6(a) and (b), respectively. The plots were fitted by using Randles equivalent circuit. A simplified Randles circuit is commonly used model, which consists of ohmic resistance (R_{ohm}) and double layer capacitance (C_{dl}) in a parallel with charge transfer resistance (R_{ct}) or polarization resistance (R_p) [35]. It is supposed that the high frequency arc were attributed to the internal distributed R_{ohm} and the contact capacitance in the granular electrode structure [36,37]. In our study, the high frequency arc was suppressed for all spectra and was not as distinct as other literature [22–26], even though impedance was measured under non-humidified condition. The reason for not having high frequency arc was the relatively small thickness of catalyst layer. Thin catalyst layer resulted in short path for migration of ions, decreasing the distributed resistance and capacitance in the granular electrode structure [38].

As mentioned, the Nyquist plot provides information regarding on the resistance component, such as R_{ohm} and R_{ct}. The R_{ohm} and the R_{ct} of MEA-C and MEA-T according to the drying time were presented in Fig. 7(a) and (b). The initial R_{ohm} of MEA-T was greater than that of MEA-C, due to the low electrical conductivity of insulating SiO_2 in the anode of MEA-T. According to drying time, both R_{ohm} of MEA-C and MEA-T increased sharply until 30 min due to the dehydration in membrane. However, as soon as the cell started producing water, the membrane was re-humidified to some extent,

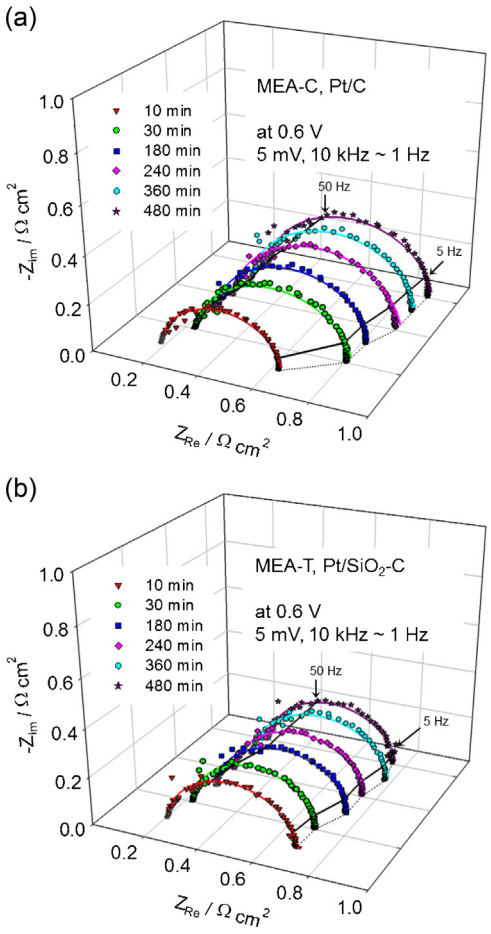

Fig. 6. The Nyquist plots during drying time from 10 min to 480 min for (a) MEA-C and (b) MEA-T.

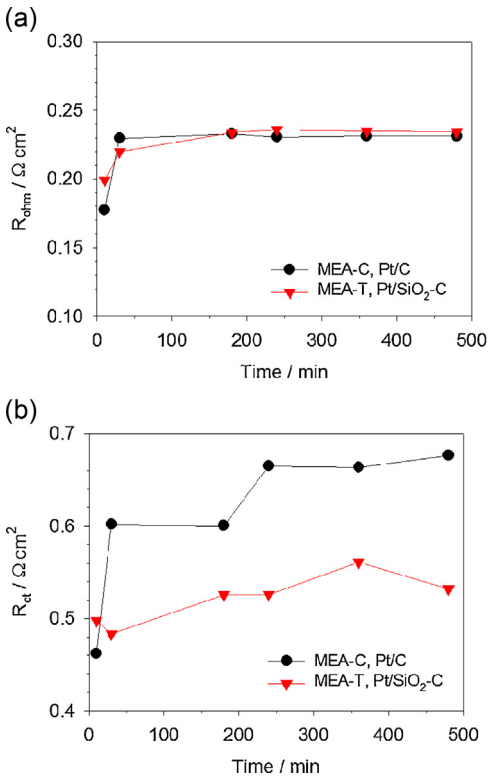

Fig. 7. (a) R_{ohm} and (d) R_{ct} extracted from the Nyquiest plot in Fig. 6 for MEA-C and MEA-T.

and the R_{ohm} became stabilized. In overall, the behavior of R_{ohm} in MEA-C and MEA-T were similar as drying, and therefore it was concluded the addition of SiO_2 in the anode of MEA-T did not affect the membrane resistance upon dehydration.

The diameter of low frequency arc represented the R_{ct} or R_p across the catalyst/electrolyte interface increases with time. The sharp increase of R_p referred the resistance change of ionomeric component. The dehydration in the catalyst layer reduced the protonic conductivity, which can be approximated by increase in R_{ct}. The extent of increase in R_{ct} of Pt/SiO_2—C is a lot smaller than Pt/C, which concluded that the Pt/SiO_2—C possessed sufficient humidity inside the anode catalyst layer, and therefore sustained the protonic conductivity. From above results, we concluded that the MEA-T was more resistance to dehydration than MEA-C owing to the self-humidifying composite catalyst. The EIS analysis for R_{ohm} and R_{ct} is a fair indication that dehydration affected mainly to the ionic conductivity of ionomer and the proton transfer within anode catalyst layer, rather than to the ionic conductivity of polymer membrane.

4. Conclusion

The authors fabricated the self-humidifying composite catalyst, which comprised of SiO_2-supported Pt and high-surfaced carbon, to keep MEA sufficiently hydrated at high temperature without external humidification for a long time. Upon ultrasonic irradiation, Pt NPs with a size of 1.4 nm was successfully formed and fixed on the surface of SiO_2 by cavitation and micro-jet effect, respectively. A variety of techniques was used to characterize the composite such as, TEM, XPS, TGA, and FE-SEM. It was revealed that 8.7 wt% of metallic Pt was included in the composite, and they were uniformly spread on the support material. The composite was employed as anode catalyst for PEMFC, and two types of MEA were prepared; a mass-corrected MEA (MEA-M) and a thickness-corrected MEA (MEA-T). Their self-humidifying abilities were evaluated and compared to Pt-only MEA (MEA-C) under non-humidified condition. The MEAs with composite catalyst exhibited stronger resistance to the dehydration than MEA-C at 70 °C with durability due to the water-retaining ability of SiO_2 in composite. Especially, MEA-T maintained 93% of initial performance after 10 h operation without humidification. Furthermore, the MEAs with composite catalyst showed higher mass-activity than the relevant studies from other research groups. The self-humidifying ability of SiO_2-supported Pt catalyst in MEA-T was examined by in-situ EIS technique in terms of the ionic resistance, and compared with MEA-C. The EIS result showed R_{ct} of MEA-T remained stable, while R_{ct} of MEA-C was greatly increased during drying. The results confirmed the lower ionic resistance of anode catalyst layer in MEA-T, due to sufficient hydration by SiO_2 in composite. The in-situ EIS characterization directly addressed that the self-humidifying ability of Pt/SiO_2—C was realized within the anode catalyst layer, and therefore the ionic conductivity of ionomer and the proton transfer was sustained at high temperature for a long time without humidification.

Acknowledgement

This work was supported by the Basic Science Research Program through the National Research Foundation of Korea funded by the Ministry of Education, Science and Technology (2011-0010369). This work was also supported by BioNano Health-Guard Research Center funded by the Ministry of Science, ICT & Future Planning (MSIP) of Korea as Global Frontier Project (Grant Number H-GUARD_2013M3A6B2078945).

Appendix A. Supplementary data

Supplementary data associated with this article can be found, in the online version, at http://dx.doi.org/10.1016/j.apcatb.2014.12.026.

References

[1] W. Vielstich, A. Lamm, H.A. Gasteiger, Handbook of Fuel Cells, Vol. 3, John Wiley & Sons, Ltd., West Sussex, England, 2003.
[2] R.P. O'hayer, S.-W. Cha, W. Colella, F.B. Prinz, Fuel Cell Fundamentals, John Wiley & Sons, Ltd. New York, NY, USA, 2006.
[3] J. Larminie, A. Dicks, Fuel Cell System Explained, John Wiley & Sons, Ltd. West Sussex, England, 2000.
[4] A. Kirubakaran, S. Jain, R.K. Nema, Renew. Sustainable Energy Rev. 13 (2009) 2430.
[5] S. Sharma, B.G. Pollet, J. Power Sources 208 (2012) 96.
[6] I. Choi, S.H. Ahn, J.J. Kim, O.J. Kwon, Appl. Catal. B-Environ. 102 (2011) 608.
[7] M. Watanabe, H. Uchida, Y. Seki, M. Emori, P. Stonehart, J. Electrochem. Soc. 143 (1996) 3847.
[8] M. Watanabe, H. Uchida, M. Emori, J. Phys. Chem. B 102 (1998) 3129.
[9] H. Hagihara, H. Uchida, M. Watanabe, Electrochim. Acta 51 (2006) 3979.
[10] H. Li, Y. Tang, Z. Wang, Z. Shi, S. Wu, D. Song, J. Zhang, K. Fatih, J. Zhang, H. Wang, Z. Liu, R. Abouatallah, A. Mazza, J. Power Sources 178 (2008) 103.
[11] K. Tuber, D. Pocza, C. Hebling, J. Power Sources 124 (2003) 403.
[12] Y. Sone, P. Ekdunge, D. Simonsson, J. Electrochem. Soc. 143 (4) (1996) 1254.
[13] T. Abe, H. Shima, K. Watanabe, Y. Ito, J. Electrochem. Soc. 151 (1) (2004) A101.
[14] K.T. Adjemian, S.J. Lee, S. Srinivasan, J. Benziger, A.B. Bocarsly, J. Electrochem. Soc 149 (3) (2002) A256.
[15] C. Bi, H. Zhang, Y. Zhang, X. Zhu, Y. Ma, H. Dai, S. Xiao, J. Power Sources 184 (2008) 197.
[16] B. Yang, Y.Z. Fu, A. Manthiram, J. Power Sources 139 (2005) 170.
[17] Y.-H. Liu, B. Yi, Z.-G. Shao, L. Wang, D. Xing, H. Zhang, J. Power Sources 163 (2007) 807.
[18] U.H. Jung, K.T. Park, E.H. Park, S.H. Kim, J. Power Sources 159 (2006) 529.
[19] W.-K. Chao, C.-M. Lee, D.-C. Tsai, C.-C. Chou, K.-L. Hsueh, F.-S. Shieu, J. Power Sources 185 (2008) 136.
[20] H.-N. Su, L.-J. Yang, S.-J. Liao, Q. Zeng, Electrochim. Acta 55 (2010) 8894.
[21] I. Choi, K.G. Lee, S.H. Ahn, D.H. Kim, O.J. Kwon, J.J. Kim, Catal. Commun. 21 (2012) 86.
[22] W. Merida, D.A. Harrington, J.M. Le Canut, G. McLean, J. Power Sources 161 (2006) 264.
[23] J.-M. Le Canut, R. Latham, W. Merida, D.A. Harrington, J. Power Sources 192 (2009) 457.

[24] B. Andreaus, A.J. McEvoy, G.G. Scherer, Electrochim. Acta 47 (2002) 2223.
[25] T.J.P. Freire, E.R. Gonzalez, J. Electroanal. Chem. 503 (2001) 57.
[26] J.-M. Le Canut, R.M. Abouatallah, D.A. Harrington, J. Electrochem. Soc. 153 (5) (2006) A857.
[27] Y. Nagata, Y. Watananabe, S. Fujita, T. Dohmaru, S. Taniguchi, J. Chem. Soc. Chem. Commun. 21 (1992) 1620.
[28] B.G. Pollet, Int. J. Hydrogen Energy 35 (2010) 11986.
[29] T. Makuta, M. Sakaguchi, H. Kusama, Mater. Lett. 77 (2012) 110.
[30] M.S. Longuethiggins, H. Oguz, J. Fluid Mech. 290 (1995) 183.
[31] C.I. Lee, S.P. Jung, H.R. Shiu, W.C. Chang, C.H. Cheng, ECS Trans. 30 (1) (2011) 217.
[32] T.-L.L. Yu, H.-L. Lin, P.-H. Su, G.-W. Wang, Open Fuels Energy Sci. J. 5 (2012) 28.
[33] J.W. Lim, Y.-H. Cho, M. Ahn, D.Y. Chung, Y.-H. Cho, N. Jung, Y.S. Kang, O.-H. Kim, M.J. Lee, M. Kim, Y.-E. Sung, J. Electrochem. Soc. 159 (4) (2012) B378.
[34] P.M. Gomadam, J.W. Weidner, Int. J. Energy Res. 29 (2005) 1133.
[35] N. Sekar, R.P. Ramasamy, J. Microbial. Biochem. Technol. S6 (2013) 1.
[36] A. Fischer, J. Jindra, H. Wendt, J. Appl. Electrochem. 28 (1998) 277.
[37] V.A. Paganin, C.L.F. Oliveira, E.A. Ticianelli, T.E. Springer, E.R. Gonzalez, Electrochim. Acta 43 (24) (1998) 3761.
[38] F. Liu, B. Yi, D. Xing, J. Yu, Z. Hou, Y. Fu, J. Power Sources 124 (2003) 81.

Update

Applied Catalysis B: Environmental
Volume 174–175, Issue , September 2015, Page 544

DOI: https://doi.org/10.1016/j.apcatb.2015.03.010

Applied Catalysis B: Environmental 174–175 (2015) 544

Contents lists available at ScienceDirect

Applied Catalysis B: Environmental

journal homepage: www.elsevier.com/locate/apcatb

Corrigendum

Corrigendum to "Characterization of self-humidifying ability of SiO_2-supported Pt catalyst under low humidity in PEMFC" [Appl. Catal. B: Environ. 168–169 (2015) 220–227]

Insoo Choi[a,b], Hyunjoon Lee[c], Kyoung G. Lee[b], Sang Hyun Ahn[d], Seok Jae Lee[b], Hyun-Jong Kim[e], Ho-Nyun Lee[e], Oh Joong Kwon[c,*]

[a] Division of Energy Engineering, Kangwon National University, 346 Jungang-ro, Samcheok, Gangwon-do 245-711, Republic of Korea
[b] Center for Nanobio Integration & Convergence Engineering (NICE), National Nanofab Center, 291 Daehak-ro, Yuseong-gu, Daejeon 305-806, Republic of Korea
[c] Department of Energy and Chemical Engineering, Incheon National University, 119 Academy-ro, Yeonsu-gu, Incheon 406-772, Republic of Korea
[d] Fuel Cell Research Center, Korea Institute of Science and Technology (KIST), 5 Hwarangno 14-gil, Seongbuk-gu, Seoul 136-791, Republic of Korea
[e] Surface Technology Center, Korea Institute of Industrial Technology (KITECH), 7-47, Songdo-dong, Incheon 406-840, Republic of Korea

The authors regret to inform that the previous author affiliation should be corrected as above. Author would like to apologize for the inconvenience caused.

DOI of original article: http://dx.doi.org/10.1016/j.apcatb.2014.12.026.
* Corresponding author. Tel.: +82 32 835 8414; fax: +82 32 835 8423.
E-mail address: ojkwon@inu.ac.kr (O.J. Kwon).

http://dx.doi.org/10.1016/j.apcatb.2015.03.010